

# INSTALLATION AND ON-LINE COMMISSIONING OF EBIS AT ATLAS\*

P.N. Ostroumov<sup>†1</sup>, A. Barcikowski, J. Clark, C.A. Dickerson, M. Hendricks, Y. Luo, R.C. Pardo, C. Peters, M. Power, G. Savard, S.I. Sharamentov, R.C. Vondrasek, G. Zinkann,  
Argonne National Laboratory, Argonne, 9700 S. Cass Av, IL 60439, USA

<sup>1</sup>also at FRIB, Michigan State University, 640 S. Shaw Lane, East Lansing, MI 48824, USA

## Abstract

An Electron Beam Ion Source Charge Breeder (EBIS-CB) has been developed at Argonne to breed radioactive beams from the Californium Rare Ion Breeder Upgrade (CARIBU) facility at ATLAS. The CARIBU EBIS-CB has been successfully commissioned offline with an external singly-charged cesium ion source [1]. The EBIS performance meets the breeding requirements to deliver CARIBU beams to ATLAS. EBIS can provide charge-to-mass ratios  $\geq 1/7$  for all CARIBU beams with breeding times in the range of 6 ms to 30 ms. A record high breeding efficiency of up to 28% into a single charge state of  $\text{Cs}^{28+}$  has been demonstrated. Following the offline testing EBIS was moved to the front end of ATLAS where the alignment of EBIS was substantially improved and additional beam diagnostic tools both for electron and ion beams were installed. This paper will discuss EBIS improvements and present the results of on-line commissioning.

## INTRODUCTION

The major features of the CARIBU EBIS are: ultra-high vacuum, high electron beam current with relatively low energy in the trap, optimized linear focusing and steering fields in the injection and extraction region, good alignment of the electron and ion beam transport system components and availability of 8 pairs of steering dipole coils for the transport of the electron beam. A typical charge state distribution of the EBIS charge-bred cesium beam downstream of a 70-degree analyzing magnet measured in off-line tests is shown in Fig. 1. The energy spread of the extracted ions has been determined by using a beam tracking code and fitting the simulated ion beam distribution to the measured data. This preliminary data indicates that for a typical beam with a mass-to-charge ratio of 4.75, the total relative energy spread at  $5\sigma$  level will be  $\sim 0.18\%$  in the ATLAS Low Energy Beam Transport (LEBT). Operation at higher repetition rates, up to 30 Hz, is dictated by the space charge limit in the radio-frequency quadrupole cooler-buncher (RFQ-CB), which precedes the EBIS-CB in the final installation, in order to maintain a high bunching efficiency. Recently, it was decided to include a multi-reflection time-of-flight (MR-TOF) mass-spectrometer between the RFQ-CB and EBIS-CB. The MR-TOF can provide isobar purification with mass resolution down to  $1/50,000$ . This paper describes the design of the new beam

transport systems and the overall integration of the EBIS-CB into ATLAS including the first experiment with breeding and acceleration of radioactive ion beam.

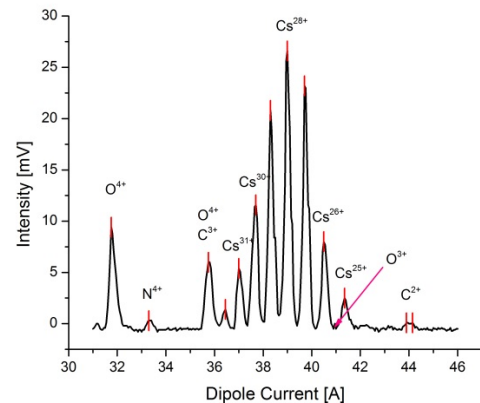


Figure 1: Typical spectrum of the EBIS beam with  $\text{Cs}^{1+}$  injection.

## EBIS INTEGRATION

The 3D layout of the EBIS High-Voltage (HV) platform with respect to CARIBU and ATLAS is shown in Fig. 2. The EBIS injection and extraction beamline components and power supplies are installed on a HV platform biased to the same potential as the CARIBU platform. In addition, the electron gun, the SC solenoid and the electron collector of the EBIS are biased with respect to the HV platform. The total accelerating voltage will be adjusted to provide a 30.5 keV/u injection energy into the ATLAS-RFQ. The details of the EBIS integration into CARIBU and ATLAS including a thorough beam optics design are given in ref. [2].

A new frame for the EBIS HV platform was constructed. Major EBIS subsystems were disassembled to move from the off-line test area to ATLAS and install on the new platform as shown in Fig. 3.

## CARIBU TO EBIS BEAMLIN

The CARIBU facility can deliver radioactive beams of singly charged ions in the mass range from 80 to 160 AMU, formed from the fission fragments of a 1 Curie  $^{252}\text{Cf}$  source. Mass separation of the beams is performed using two  $60^\circ$  dipole magnets. The mass separator is followed by the RFQ-CB which provides cooling and bunching of the beam [3]. Recently, a Multi-Reflection Time of Flight (MR-TOF) spectrometer and mass separator has been installed downstream of the RFQ-CB. The mass resolving power of the MR-TOF can reach up to

\* This work was supported by the U.S. Department of Energy, Office of Nuclear Physics, under Contract DE-AC02-06CH11357. This research used resources of ANL's ATLAS facility, which is a DOE Office of Science User Facility.

<sup>†</sup> Ostroumov@frib.msu.edu

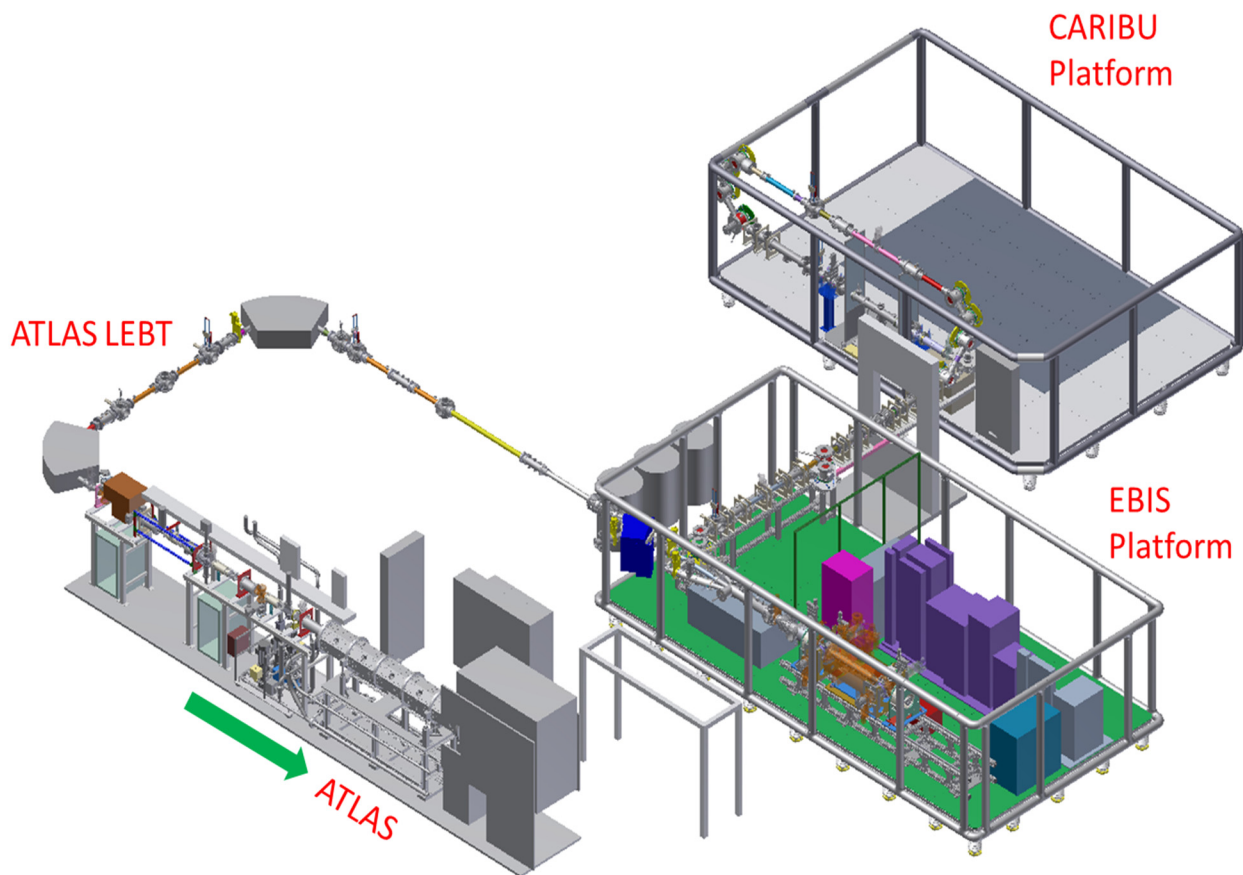


Figure 2: 3D layout of the ATLAS front-end with the EBIS charge breeder.



Figure 3: General view of the EBIS.

$5 \cdot 10^4$  for the period of time between the charge breeding cycles in the EBIS. The high mass resolving power is achieved for short beam pulses below  $1 \mu\text{s}$ . To deliver beam from the MR-TOF to EBIS, we have designed an all-electrostatic beam transport system. The main goal of the beam optics design was the minimization of the emittance distortions due to aberrations and beam energy spread. Due to the very limited space, the beam is bent by  $180^\circ$  in the vertical plane immediately after the extraction from the MR-TOF as is shown in Fig. 2 and 4. The deflection of the low-energy,  $\sim 5 \text{ keV}$ , beam by a substantial angle is challenging due to the high geometrical emittance and relative energy spread. Spherical electrostatic  $45^\circ$  benders were designed to achieve isochronous beam transport with minimal emittance growth through two  $180^\circ$  bends. Immediately following the  $180^\circ$  vertical bend after the MR-TOF, the beam is accelerated to higher energy to match the EBIS injection-extraction beamline which is designed to accept up to  $50 \text{ keV}$  beams [4]. While DC acceleration is possible, it would require the addition of a floating potential with a significant amount of equipment. To avoid that, a pulsed acceleration is employed in the two-gap pulsed accelerator (PA) shown in Fig. 4. In the PA, the ions are accelerated in the first accelerating gap and then enter a long drift tube. While the ion bunch is inside the drift tube the voltage of the tube is switched to a positive potential using a fast Behlke switch, so the ions are accelerated again in a second accelerating gap when they exit the tube. The length of the center drift tube was chosen to be  $70 \text{ cm}$  in order to accommodate bunches with  $\Delta t \leq 2.5 \mu\text{s}$ .

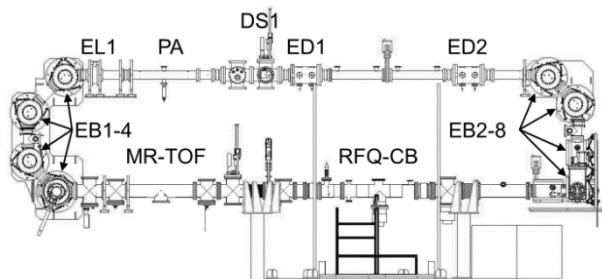


Figure 4: Side view of the beam transport system installed on the CARIBU platform. EB1-8 -  $45^\circ$  spherical electrostatic benders; EL1 - Einzel lens; PA - Two-step Pulsed Accelerator; DS1 - Diagnostics Station; ED1-2 - Electrostatic Doublets.

After the second vertical bend, the beam is brought to the original height and rotated by  $90^\circ$  towards the EBIS platform (see Fig. 2). The top view of the CARIBU-EBIS beamline is shown in Fig. 5. Four electrostatic doublets (ED3-6) are used to create an inverse transformation in front of the EB9 and an identity transformation upstream of the EB11. EB9-10 will be used in the future for beam delivery to low energy experiments. The injection-extraction line of the EBIS was thoroughly described in ref. [4] and it is included in our simulations. Fig. 6 displays the beam envelopes along the CARIBU-EBIS beamline obtained with the TRACK code [5]. The simulations were

performed with the initial beam emittance exceeding the expected emittance from the RFQ-CB by a factor of 6. The transport system provides good beam matching with the EBIS acceptance.

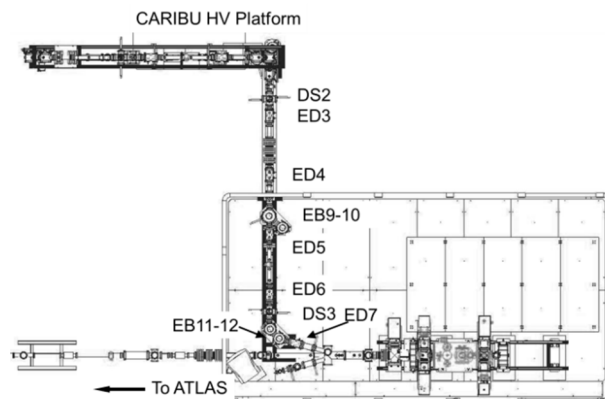


Figure 5: CARIBU to EBIS beam line. DS2 - Diagnostics Station; ED3-7 - Electrostatic Doublets; EB9-12 -  $45^\circ$  spherical electrostatic benders.

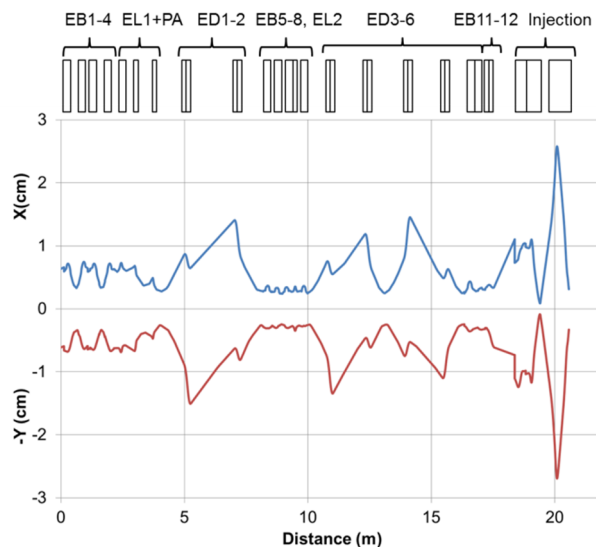


Figure 6: Beam envelopes in the CARIBU to EBIS beamline. EB - electrostatic benders, EL - Einzel lenses; ED - electrostatic doublets; PA - pulsed accelerator.

## EBIS TO ATLAS LEBT

The existing ATLAS LEBT has been modified to include only electrostatic focusing quadrupoles and to provide three main functions:

- Selection of the charge states of the radioactive ions extracted from the EBIS with maximized mass resolving power.
- A focused and axially symmetric beam at the location of the Multi-Harmonic Buncher (MHB).
- Achromatic beam transport to avoid emittance growth due to the energy spread.

TRACK [5] simulations were performed in order to optimize the mass resolving power and study its dependence on beam parameters. For typical EBIS beam parameters the

mass resolving power is  $\sim 200$ . The achromatic properties of two  $90^\circ$  magnets are provided by adding two large-aperture electrostatic quadrupole doublets located next to the magnets (see Fig. 2). A small beam size is formed in the MHB and appropriate beam matching into the RFQ is provided [2]. There are no beam losses and no emittance growth along the LEBT.

### BEAM DIAGNOSTICS

A set of beam diagnostics tools have been designed, built and installed in the CARIBU-EBIS and LEBT beamlines. The beam diagnostics system allows us to tune beam transport lines both for stable ion guide beams and radioactive low-intensity beams. Charge bred residual gas or stable  $^{133}\text{Cs}$  injected from a dedicated surface ionization source are used as guide beam in the EBIS to ATLAS LEBT. The beam diagnostics system includes:

- Shielded Faraday Cups (FC). Both signal and bias electrodes are well shielded and grounded to the beam pipe to reduce the background noise.
- FCs based on multichannel plates (MCP). This FC measures the intensity of secondary electrons created by ions bombarding the MCP.
- Pepper-pot emittance probes with MCPs. The image of secondary electrons on a phosphor screen is used to extract the beam emittance. The secondary electrons are created by ions bombarding the MCP.
- Annular MCPs. The primary ion beam generates secondary electrons from an aluminium target. The electrons are accelerated backwards and collected by the annular MCP.
- Silicon detectors for the measurement of radioactive beam intensity by counting  $\beta$ -decay events.

### EBIS BEAM ACCELERATION IN ATLAS

The installation of the EBIS and the LEBT section connecting it to the ATLAS followed by sub-system check-out and interlocks testing were completed in April 2016. The initial EBIS commissioning and first beam acceleration in the Positive Ion Injector (PII) up to 1.84 MeV/u were performed using  $^{16}\text{O}^{6+}$  beam created from the residual gas in the EBIS trap. The oxygen beam extracted from the EBIS trap in a pulsed mode with 1 Hz repetition rate was successfully accelerated in ATLAS. The main goal of the experiments was to accelerate beam through PII with a good efficiency. This goal was achieved and transmission efficiency was measured to be 75.4% while the theoretical value is 83%. Figure 7 shows the oxygen beam signal from the FC located after the PII. The pulsed signal is integrated due to the cable capacitance of 126 pF. The collected charge corresponds to  $2.2 \cdot 10^6$  oxygen ions per pulse.

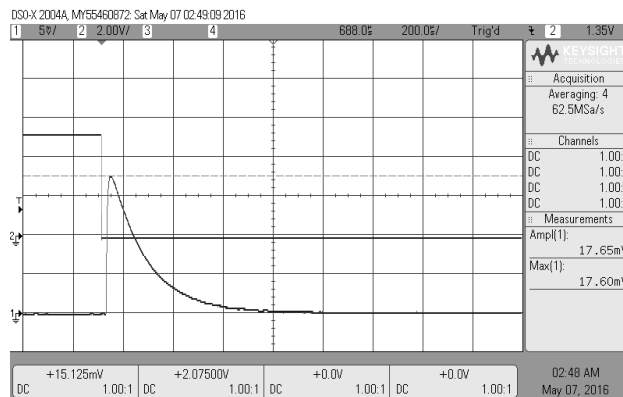


Figure 7: Oxygen 6+ beam signal from the FC located at the exit of PII section of ATLAS.

In the following months, the EBIS has been operated at a 10 Hz repetition rate with a cesium beam.

### BREEDING AND ACCELERATION OF RARE ISOTOPES

The installation of the beamline connecting CARIBU to EBIS was completed in August 2016. The section of the beamline connecting CARIBU platform with the EBIS platform is shown in Fig. 8. The LEBT and accelerator were tuned utilizing a charge bred beam of  $^{133}\text{Cs}^{26+}$ . A 40  $\mu\text{s}$  pulse of  $^{133}\text{Cs}^{26+}$  was produced by a surface ionization source and charge bred for 24 ms with an electron beam current of 1.15 A running with a repetition rate of 2 Hz.

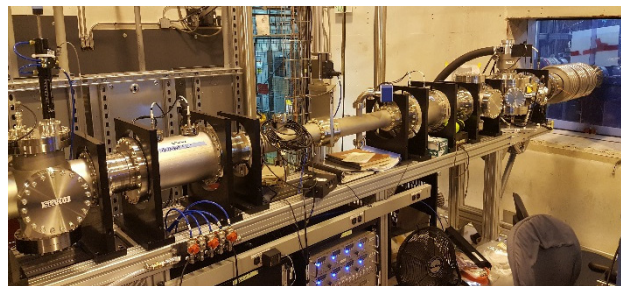


Figure 8: The section of the beam line connecting CARIBU with EBIS.

The  $^{133}\text{Cs}^{26+}$  was tuned through the LEBT and accelerated in the RFQ and PII linac to an energy of 215 MeV as shown in Fig. 9. The beam was observed with the energy diagnostics at the PII exit consisting of a 50  $\mu\text{g}/\text{cm}^2$  gold scattering foil and a silicon barrier detector (at 0 degree). There was sufficient beam intensity that it could be observed with a Keithley femtoammeter. Transmission of the  $^{133}\text{Cs}^{26+}$  from the EBIS exit to the exit of the linac was 23% with the majority of the loss occurring between the exit of the EBIS and the first FC after the mass analysis. The beam transmission is summarized in Table 1. The goal of these experiments was to demonstrate the breeding of radioactive ions and acceleration in ATLAS.

Table 1:  $^{133}\text{Cs}$  Beam Transmission

FC location	Beam current (epA)
EBIS Deck	3.2
After analysing slits	1.21
Upstream of the RFQ	0.92
After PII	0.73

Therefore, there was not sufficient time to improve the transmission from the EBIS to the mass analysing slits. The overall transmission efficiency can be potentially increased by a factor of 3.5 which will be achieved in the following accelerator experiments with CARIBU beams.

After tuning the  $^{133}\text{Cs}^{26+}$ , the LEBT and accelerator were scaled to radioactive ions,  $^{142}\text{Cs}^{28+}$ . The high voltage deck was set to velocity match into the RFQ. The tune was checked by scaling the two ground dipoles back to the  $^{133}\text{Cs}^{26+}$  settings and confirming beam transmission through the LEBT. We then re-established the  $^{142}\text{Cs}^{28+}$  tune and looked at the background spectrum. The spectrum showed contaminants of K-41, Zn-66, I-127, Ce-142, and potentially Ir-193 (see Fig. 10). The rate observed in the energy detector was 1 Hz with the detector at 1 degree. For comparison, the typical background rate observed from the ECR charge breeder was  $\sim 1$  kHz. These measurements confirm a very important property of the EBIS: very low contamination of the primary radioactive beam with stable isotopes. The e-gun cathode is made of IrCe which explains the origin of iridium and cerium in the spectrum.

Transmission of the  $^{142}\text{Cs}^{28+}$  beam from the EBIS deck to the first mass analysis point was  $\sim 40\%$ .

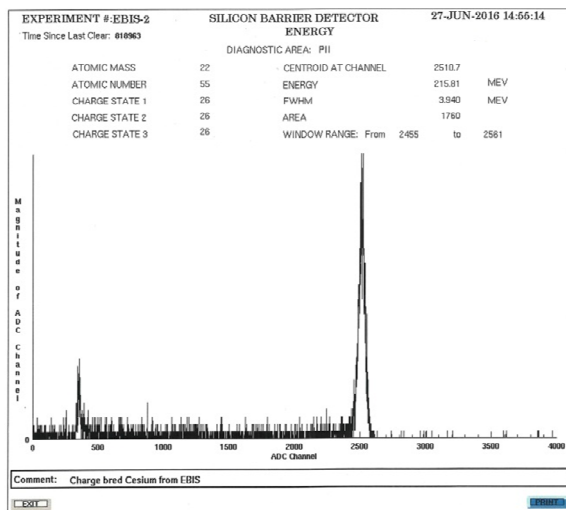


Figure 9:  $^{133}\text{Cs}^{26+}$  beam energy measurement after the PII with a silicon barrier detector.

We then tuned the EBIS for the best transmission utilizing only the injection elements so that the extraction tune into the LEBT was preserved. The best  $^{142}\text{Cs}$  transmission efficiency through EBIS was 42%. This is in line with the 40% transmission efficiency observed with the  $^{133}\text{Cs}$ . The charge state distribution of  $^{142}\text{Cs}$  after breeding is shown in Table 2.  $^{142}\text{Cs}$  was peaked on 27+.

Table 2:  $^{142}\text{Cs}$  Charge State Distribution

Charge state	25+	26+	27+	28+
Count rate (Hz)	8.75	15.5	18.25	14.5

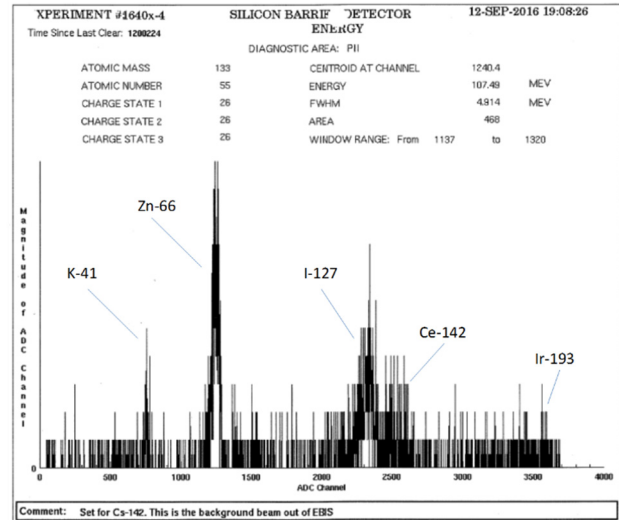


Figure 10: The energy spectrum of background ions at the exit of PII.

## CONCLUSION

The Electron Beam Ion Source was successfully integrated with CARIBU and EBIS. The singly charged radioactive beam,  $^{142}\text{Cs}^{1+}$ , was transported to EBIS with matching injection energy and charge bred to  $^{142}\text{Cs}^{28+}$  with an efficiency of 10%. One of the main properties of the EBIS is very low contamination of the accelerated radioactive ions. This property was immediately confirmed when the LEBT and PII were tuned for acceleration of radioactive ions and accelerated background ions were measured without injection of radioactive ions into EBIS. As expected there were multiple occasions of unstable operation of some hardware inherent to the beam commissioning stage. The transmission efficiency and availability of the accelerated radioactive beams will be significantly improved in the next accelerator run in upcoming weeks.

## REFERENCES

- [1] P. N. Ostroumov, A. Barcikowski, C. A. Dickerson, A. Perry, A. I. Pikin, S. I. Sharamentov, R. C. Vondrasek and G. P. Zinkann, *Rev. Sci. Instrum.* 86, 083311 (2015); <http://dx.doi.org/10.1063/1.4929464>
- [2] Perry, PhD Thesis, Illinois Institute of Technology, August 2015.
- [3] Savard, S. Baker, C. Davids, A.F. Levand, E.F. Moore, R.C. Pardo, R. Vondrasek, B.J. Zabransky, and G. Zinkann, *Nucl. Instrum. Methods Phys. Res. Sect. B* 266, 4086 (2008).
- [4] Dickerson, B. Mustapha, S. Kondrashev, P. N. Ostroumov, and G. Savard, *Rev. Sci. Instrum.* 83, 02A503 (2012).
- [5] P.N. Ostroumov, V. Aseev, and B. Mustapha, *Phys. Rev. ST. Accel. Beams*, Volume 7, 090101 (2004).